Journal of
Plant Ecology

VOLUME 4, NUMBER 4,
PAGES 302–312

DECEMBER 2011

doi: 10.1093/jpe/rtr019

Advanced Access published
on 11 July 2011

available online at
www.jpe.oxfordjournals.org

Application of two remote sensing GPP algorithms at a semiarid grassland site of North China

Jianfeng Liu[1,2,3], *Osbert Jianxin Sun*[4,5,*], *Hongmei Jin*[6], *Zhiyong Zhou*[4,5] *and Xingguo Han*[1]

[1] *State Key Laboratory of Vegetation and Environmental Change, Institute of Botany, Chinese Academy of Sciences, Beijing 100093, People's Republic of China*
[2] *Research Institute of Forestry, Chinese Academy of Forestry, Beijing 100091, People's Republic of China*
[3] *Graduate University of Chinese Academy of Sciences, Beijing 100049, People's Republic of China*
[4] *Institute of Forestry and Climate Change Research, Beijing Forestry University, Beijing 100083, People's Republic of China*
[5] *MOE Key Laboratory for Silviculture and Conservation, Beijing Forestry University, Beijing 100083, People's Republic of China*
[6] *Institute of Agricultural Resources and Environment, Jiangsu Academy of Agricultural Sciences/Jiangsu Agricultural Waste Treatment and Recycle Engineering Research Center, Nanjing 210014, People's Republic of China*
*Correspondence address. Institute of Forestry and Climate Change Research, Beijing Forestry University, 35 Qinghua East Road, Haidian District, Beijing 100083, China. Tel: +86-10-6233-7095; E-mail: sunjianx@bjfu.edu.cn

Abstract

Aims
Estimation of gross primary production (GPP) from remote sensing data is an important approach to study regional or global carbon cycle. However, for a given algorithm, it usually has its limitation on applications to a wide range of vegetation types and/or under diverse environmental conditions. This study was conducted to compare the performance of two remote sensing GPP algorithms, the MODIS GPP and the vegetation photosynthesis model (VPM), in a semiarid temperate grassland ecosystem.

Methods
The study was conducted at a typical grassland site in Ujimuqin of Inner Mongolia, North China, over 2 years in 2006 and 2007. Environmental controls on GPP measured by the eddy covariance (EC) technique at the study site were first investigated with path analysis of meteorological and soil moisture data at a daily and 8-day time steps. The estimates of GPP derived from the MODIS GPP and the VPM with site-specific inputs were then compared with the values of EC measurements as ground truthing at the site. Site-specific ε_{max} (α) was estimated by using rectangular hyperbola function based on the 7-day flux data at 30-min intervals over the peak period of the growing season (May to September).

Important Findings
Between the two remote sensing GPP algorithms and various estimates of the fraction of absorbed photosynthetic active radiation (FPAR), the VPM based on FPAR derived from the enhanced vegetation index (EVI) works the best in predicting GPP against the ground truthing of EC GPP. A path analysis indicates that the EC GPP in this semiarid temperate grassland ecosystem is controlled predominantly by both soil water and temperature. The site water condition is slightly better simulated by the moisture multiplier in the VPM than in the MODIS GPP algorithm, which is a most probable explanation for a better performance of the VPM than MODIS GPP algorithm in this semiarid grassland ecosystem.

Keywords: MODIS GPP • VPM • eddy covariance • path analysis • grassland

Received: 21 November 2010 Revised: 6 May 2011 Accepted: 6 June 2011

INTRODUCTION

Gross primary production (GPP), which is the sum of photosynthetic carbon uptake by vegetation, is one of the fundamental variables in the global carbon balance. However, because of the spatial extent, it would be extremely labor intensive and economically costly to estimate GPP at regional scale based on biological measurements in the field. With rapid advancement of remote sensing technology, it has become a common practice to utilize parameters derived

from remote sensing data to estimate GPP at a regional or global scale.

There are various types of remote sensing products that offer parameters such as classification of vegetation type and normalized difference vegetation index (NDVI), or other vegetation indices (Xie *et al.* 2008), for use in the estimation of GPP based on modeling approach. MODIS GPP algorithm, i.e. MOD17, is a type of light use efficiency (LUE) model developed for predicting global GPP with the remote sensing imagery of moderate spatial resolution (~1 km) and high temporal frequency (8 day) (Running *et al.* 2004). However, it may over- or underestimate ecosystem GPP with varying climatic conditions and vegetation types because of the algorithm inputs, including the climate input data, the FPAR (fraction of photosynthetic active radiation [PAR] absorbed by the canopy) and the base rate for light use efficiency (Turner *et al.* 2006). Lack of explicit representation on soil water constraint within the MODIS GPP algorithm usually leads to GPP overestimation for water-limiting ecosystems (Coops *et al.* 2007; Fensholt *et al.* 2006; Leuning *et al.* 2005). Moreover, the FPAR in the MODIS algorithm is generally derived from empirical relationships or radiation transfer models (Knyazikhin *et al.* 1999) and has been found to be overestimated for semiarid ecosystems (Fensholt *et al.* 2004; Turner *et al.* 2005).

Based on the conceptual partitioning of chlorophyll and non-photosynthetic active vegetation (NPV) within a canopy, Xiao *et al.* (2004a) developed the vegetation photosynthesis model (VPM) for estimation of GPP over the photosynthetic active period of vegetation. It has been applied for estimating GPP in forests (Wu *et al.* 2009; Xiao *et al.* 2004a, 2004b, 2005a, 2005b), grasslands (Li *et al.* 2007; Wu *et al.* 2008) and croplands (Yan *et al.* 2009) and is found to provide better estimates of GPP than the corresponding MOD17 product (Wu *et al.* 2008; Xiao *et al.* 2004b). The enhanced vegetation index (EVI, Huete *et al.* 1997), which functions as FPAR in the VPM, has been demonstrated to be more sensitive to canopy variation than NDVI (Huete *et al.* 2002; Xiao *et al.* 2004b).

Despite the increasing development of various approaches in assessing ecosystem productivity based on remote sensing data, uncertainty remains on how appropriate a given set of algorithms can be in application to specific ecosystems under specific environmental conditions. For example, in the grassland ecosystems of North China, different methods have been used to derive productivity based on remote sensing data, e.g. MODIS GPP (Qin *et al.* 2004), VPM (Li *et al.* 2007; Wu *et al.* 2008), CASA (Zhang *et al.* 2008), but outcome of the model performance varies among the different approaches. The use of CASA, which is an ecoprocessed model, is constraint by difficulties in obtaining complex driving variables; the MODIS GPP (MOD17) is shown to overestimate grass production compared with values based on ground sampling (Qin *et al.* 2004), while the VPM GPP predictions compare well with the observed GPP using the eddy covariance (EC) technique (Li *et al.* 2007; Wu *et al.* 2008).

Globally, the MODIS GPP and VPM algorithm are both recognized for having a great potential for estimating productivity over a wide range of ecosystem types because of their robust performance and general availability of required data sources (Running *et al.* 2000; Xiao *et al.* 2004a, 2004b, 2005a, 2005b). However, how well the two algorithms compare in application to a fixed site is yet to be tested. This study was therefore conducted to compare the performance of the MODIS GPP and VPM in estimating productivity at the site level, with GPP measurements by the EC technique as the ground truthing, based on 2 years of data at a typical grassland site in Ujimuqin of Inner Mongolia, North China.

MATERIALS AND METHODS

Study site

The study was conducted on a typical steppe site (lat. 45.560°N, long. 117.000°E) situated in East Ujimuqin of Inner Mongolia, North China. The general conditions of the study area are as described in detail in Jin *et al.* (2010) and Shao *et al.* (2008). The vegetation is dominated by *Stipa krylovii* Roshev., *Leymus chinensis* (Trin.) Tzvel., *Carex duriuscula* C.A. Mey, *Cleistogenes squarrosa* (Trin.) Keng, with minor species including *Chenopodium glaucum* Linn., *Agropyron cristatum* Linn. and *Artemisia frigida* Willd. The climate is of continental and monsoon type with long-term (1956–2005) mean annual air temperature at 1.2°C and rainfall at 257.7 mm. Base soils in this region are of calcic–orthic Aridisol (Jin *et al.* 2010).

The study area suffered severe drought in both 2006 and 2007. The sum of precipitation (May to September) was only about half of that averaged over the previous 50 years, and the air temperature increased by 1.6°C in 2006 and 3.6°C in 2007 over the long-term average (Fig. 1).

An open-path EC system was established in July 2005. Measurements were made during growing season (from May to October) in both 2006 and 2007.

Overview of remote sensing GPP algorithms

MODIS GPP

The MODIS GPP algorithm is described in detail by Heinsch *et al.* (2003) and Running *et al.* (2004). In brief, the algorithm is based on the radiation conversion efficiency concept of Monteith (1972). MODIS-derived estimates of FPAR and independent estimates of PAR are transformed using a light use efficiency factor, ε, to compute GPP (Heinsch *et al.* 2003, 2006; Running *et al.* 2004; Zhao *et al.* 2005). ε is reduced from ε_{max} (the biome-specific maximum conversion efficiency) when daily minimum temperature and vapor pressure deficit (VPD) are less than optimal. A single ε_{max} value is assigned to each of 12 broad land cover classes recognized in the MOD-12 University of Maryland classification. The resulting Biome Properties Look-Up Table (BPLUT) contains values specifying minimum temperature and VPD limits, specific leaf area and respiration coefficients for the standard land cover classes (Heinsch *et al.* 2003).

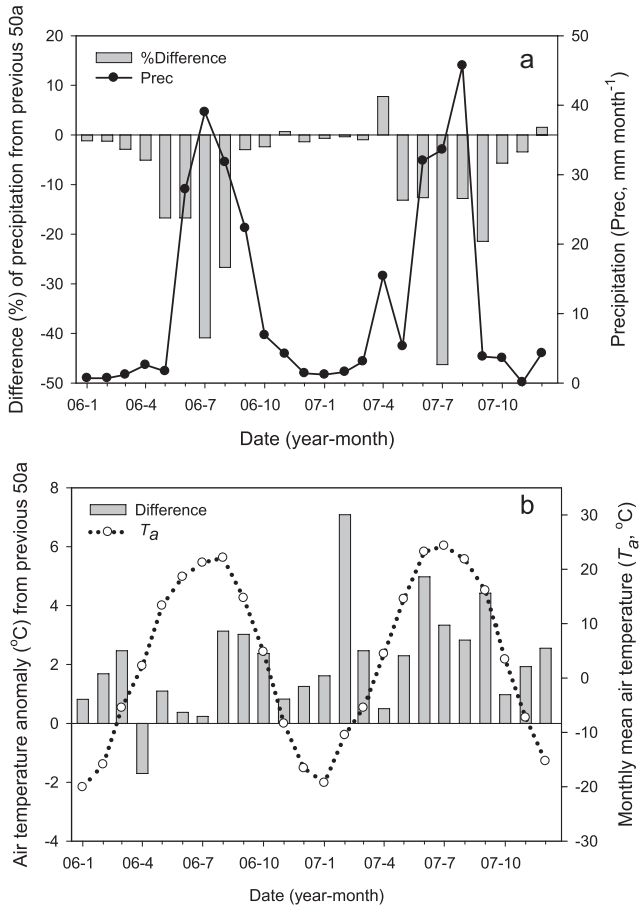

Figure 1: monthly precipitation and air temperature in 2006 and 2007 and their departures from the means of the previous 50 years (1956–2005) at the study site of East Ujimuqin of Inner Mongolia, China.

VPM GPP

The satellite-based VPM is developed by Xiao *et al.* (2004a) to estimate GPP of terrestrial ecosystems. It is also an LUE model similar to the MODIS GPP algorithm, but its FPAR is partitioned into the fraction of PAR absorbed by chlorophyll ($FPAR_{chl}$) and by non-photosynthetic active components ($FPAR_{npv}$). The former is used to calculate GPP and estimated as a linear function of EVI (Huete *et al.* 1997). ε_{max} is estimated from site flux data and accounts for the effects of temperature (T_{scalar}), water (W_{scalar}) and leaf phenology (P_{scalar}). T_{scalar} is estimated by using the equation developed for the Terrestrial Ecosystem Model (Raich *et al.* 1991). W_{scalar} and P_{scalar} are estimated by the LSWI (Xiao *et al.* 2002). But for grassland, the P_{scalar} is set to 1, without considering the effect of leaf age on photosynthesis (Li *et al.* 2007). The equations of MODIS GPP and VPM are summarized in the Appendix.

EC GPP

The EC technique greatly facilitates the estimates of GPP over various ecosystems. At our study site, the daily flux data of net ecosystem CO_2 exchange (*NEE*), ecosystem respiration and GPP were generated from the half-hourly flux data collected during the growing seasons (May to September) of 2006 and 2007. Webb–Pearman–Leuning corrections and three-dimension coordinate rotations were made to correct for the density and tilt effects (Webb *et al.* 1980; Wilczak *et al.* 2001). Anomalous or spurious values caused by sensor malfunction and rain events were removed from the datasets. NEE data of the friction velocity (U^*) $\leqslant$ 0.2 m/s during nighttime were also rejected. Gap filling of missing data were achieved using different strategies. For gaps $\leqslant$2 h, the missing data were linearly interpolated. For large gaps (>2 h), the missing daytime NEE data were estimated as a function of PAR with the Michaelis–Menten equation (Falge *et al.* 2001, A.8), with coefficients fitted on a weekly basis. The nighttime data gaps were filled by using the empirical relationships between ecosystem respiration and soil temperature under high turbulence (Lloyd and Taylor 1994). The resultant regression equation was then used to predict ecosystem respiration during daytime (solar altitude > 0) based on measured soil temperature. GPP was derived by subtracting the daytime ecosystem respiration (R_{eco_d}) from the corresponding daytime NEE. Daily GPP data were aggregated to 8-day intervals to be consistent with the MODIS 8-day composites.

Data sources

Site-specific 8-day MODIS GPP (MOD17A2, C5) and FPAR (MOD15A2, named FPAR_MOD15) data (spatial resolution 1-km) over the growing seasons of 2006 and 2007 were acquired from the Oak Ridge National Laboratory Distributed Active Archive Center (http://daac.ornl.gov/MODIS/modis.html), together with the vegetation indices such as NDVI, EVI and LSWI derived from the MODIS Land Surface Reflectance product (MOD09A1, spatial resolution 500 m) (Huete *et al.* 1997; Tucker 1979; Xiao *et al.* 2002). Estimates of FPAR were derived from both EVI (FPAR_EVI, namely EVI) and NDVI (FPAR_NDVI). FPAR_NDVI were generated by a backup algorithm based on biome-specific empirical relationships between the NDVI and FPAR described in detail in Knyazikhin *et al.* (1999). All above satellite-based data were extracted from the MODIS imagery centered on the flux tower, based on the geolocation information (latitude and longitude) of the flux tower site.

The maximum light use efficiency (ε_{max}) varies with vegetation types, and for a specific vegetation type, it can be obtained from a survey of the literature and/or analysis of nearly instantaneous NEE of CO_2 and PAR at a CO_2 eddy flux tower site based on a linear or a non-linear regression (Goulden *et al.* 1997; Xiao 2006). In this study, site-specific ε_{max} (α) was estimated by using rectangular hyperbola function (Michaelis–Menten equation, Falge *et al.* 2001; Li *et al.*2007; Yan *et al.*2008) based on the 7-day flux data at 30-min intervals over the peak period of the growing season (May to September) in 2006 and 2007. For the calculated ε_{max} time series with 7-day intervals in East Ujimuqin, the maximum value of ε_{max} occurs in the middle of July or August in both 2006 and 2007

(Table 1). The same maximum ε_{max} estimates were used over the two growing seasons for the two GPP algorithms. T_{min}, T_{max} and T_{opt}, which are set as 0, 35 and 20°C, respectively, were used to calculate T_{scalar} of VPM.

Statistical analyses

To evaluate the dependence of the EC GPP on environmental variables at daily and 8-day intervals, we performed path analysis (Li 1981) on EC data collected during the growing season (May to September) of 2006 and 2007. Path analysis is an extension of multiple regressions and can be used to provide estimates of the magnitude and significance of hypothesized causal connections among variables (Huxman *et al.* 2003; Ignace and Huxman 2009; Saito *et al.* 2009; Sarr and Hibbs 2007; Whittaker *et al.* 2009). In this study, we focused on the following four environmental variables: air temperature (T_a) at a height of 2 m, volumetric soil water content (VWC) to a depth of 10 cm, PAR and VPD.

To assess the performance of the two remote sensing GPP algorithms as compared with the EC GPP, analysis of linear regression and *t*-test for independent samples were carried out with SPSS (v. 16.0).

RESULTS

The VPM predictions of GPP in 2006 and 2007 at an 8-day time step using site-specific meteorology and various estimates of FPAR (i.e. FPAR_EVI, FPAR_NDVI and FPAR_MOD15) were all closely related with the corresponding EC GPP (Figs 2 and Fig. 3a). However, only the VPM GPP based on the FPAR_EVI was consistent with the values of the EC GPP (Fig. 2a). The coefficient of determination, R^2, reaches 0.88 ($P < 0.001$) for the relationship between the EC GPP and the VPM GPP based on FPAR_EVI at an 8-day time step (Table 2). A *t*-test for independent samples indicates that the two sets of observations are highly similar ($P < 0.001$) with an SE of 2.423 g C m^{-2} 8 day^{-1}. When using both FPAR_NDVI and FPAR_MOD15 in the calculations, however, the VPM significantly ($P < 0.05$) overestimates GPP compared with the EC GPP (Fig. 2b and c) despite the close relationships (R^2 = 0.89 and 0.80, SE = 2.431 and 3.262 g C m^{-2} 8 day^{-1}, respectively, $P < 0.001$).

The MODIS GPP had better relationships with the EC GPP when calculated using FPAR_EVI (R^2 = 0.86, $P < 0.001$, SE = 2.799 g C m^{-2} 8 day^{-1}) and FPAR_NDVI (R^2 = 0.89, $P < 0.001$, SE = 2.386 g C m^{-2} 8 day^{-1}) than FPAR_MOD15 (R^2 = 0.79, $P < 0.001$, SE = 3.394 g C m^{-2} 8 day^{-1}) (Table 2). However, all the three calculations of the MODIS GPP produced highly biased values compared with the EC GPP; calculation based on FPAR_EVI significantly ($P < 0.01$) underestimates GPP (Fig. 2d), whereas those based on FPAR_NDVI (Fig. 2e) and FPAR_MOD15 (Fig. 2f) yield significant overestimations ($P < 0.01$) (Fig. 3b). The standard MODIS product of GPP (MOD17A2) extracted according to the geographical location of the study site also tends to negatively depart from the EC GPP ($P < 0.001$, Fig. 2g).

A simple path analysis was used to examine the relative causality of four major environmental variables in the control of GPP variability measured by the EC technique at a daily and 8-day time step. VWC and T_a had much higher values of path coefficients than PAR and VPD (Fig. 4b). Among the four variables, VWC, T_a and PAR displayed significant and positive effect on the EC GPP ($P < 0.05$). VWC displays dominant effects at the middle stage of the growing season on GPP, while T_a is dominant at the previous and late stage of the growing season (Fig. 4a).

We found that the variations in the EC GPP data were better explained by the FPAR_EVI than both the FPAR-MOD15 and FPAR_NDVI (Fig. 3c and Fig. 5). The two remote sensing GPP algorithms performed the same in the temperature multipliers (Fig. 6a), but their moisture multipliers highly contrasted in explaining the variations in the EC GPP data (Fig. 6b). Moreover, W_{scalar} in the VPM exhibited a significantly positive relationship with the VWC at the study site ($P < 0.05$), whereas VPD' in the MODIS GPP algorithm did not display any apparent pattern (Fig. 7).

Table 1: parameters of the Michaelis–Menten equation

	2006	2007
Day of year	192–199	225–232
ε_{max} ($mgCO_2$ $mmol^{-1}$)	1.317	0.993
Maximum light saturation photosynthesis rate ($mgCO_2$ m^{-2} s^{-1})	0.1806	0.1062
Adjusted R^2	0.442	0.233
n	169	169

DISCUSSION

Between the two remote sensing GPP algorithms and various estimates of FPAR, the VPM based on FPAR derived from the EVI works the best in predicting GPP against the ground truthing of EC GPP at the semiarid grassland site in East Ujimuqin of Inner Mongolia, China. A path analysis indicates that the daily or 8-day GPP at the site strongly depends on the corresponding VWC and T_a during the growing seasons. It has been suggested that controls over GPP during the growing season are identical to those for net photosynthesis of individual leaves (Chapin *et al.* 2002) as temperature and drought stress may induce the closure of stoma and result in the depression or even suspension of leaf photosynthesis. For arid or semiarid grasslands of the mid- or high-latitude characterized with low precipitation and frequent droughts (Schlesinger *et al.* 1990), soil moisture and temperature over the growing season are recognized as the predominant controls of photosynthesis and primary production (Li *et al.* 2008; Wang *et al.* 2008; Yuan *et al.* 2007).

Apart from the prediction of GPP by VPM based on FPAR_EVI, other calculations either over- or underestimate GPP. The GPP predictions extracted from the standard MOD17 product

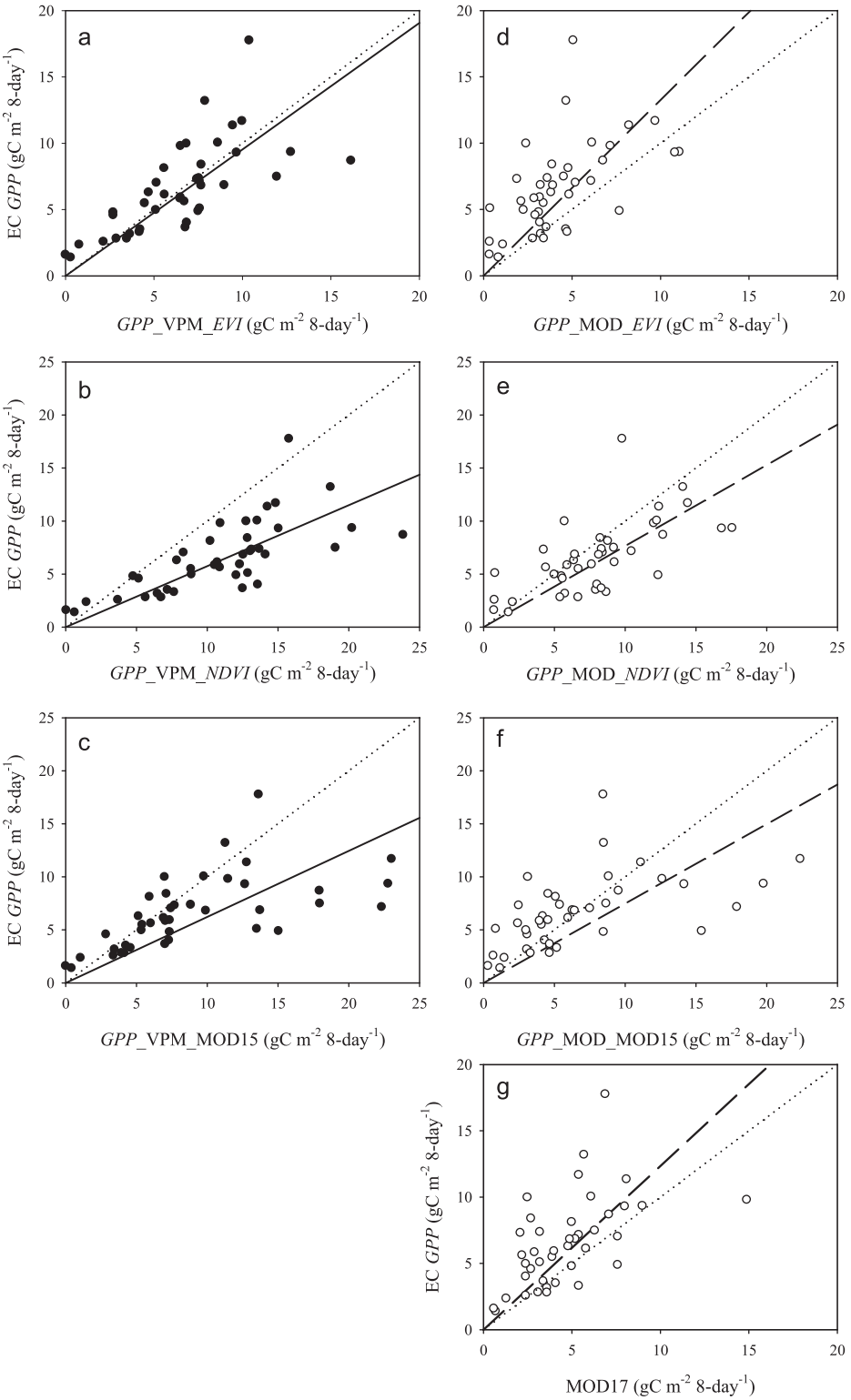

Figure 2: comparisons of the 8-day GPP measured by EC technique (EC GPP) with (**a**) the VPM predictions of GPP based on FPAR_EVI (GPP_VPM_EVI), (**b**) the VPM predictions of GPP based on FPAR_NDVI (GPP_VPM_NDVI), (**c**) the VPM predictions of GPP based on FPAR_-MOD15 (GPP_VPM_MOD15), (**d**) the MODIS predictions of GPP based on FPAR_EVI (GPP_MOD_EVI), (**e**) the MODIS predictions of GPP based on FPAR_NDVI (GPP_MOD_NDVI), (f) the MODIS predictions of GPP based on FPAR_MOD15 (GPP_MOD_MOD15) and (**g**) the standard MODIS product (MOD17A2, C5) extracted by the geographical location of the study site, in East Ujimuqin of Inner Mongolia, China. In each graph, the dash or solid line is the best linear fit and doted line is the 1:1 reference.

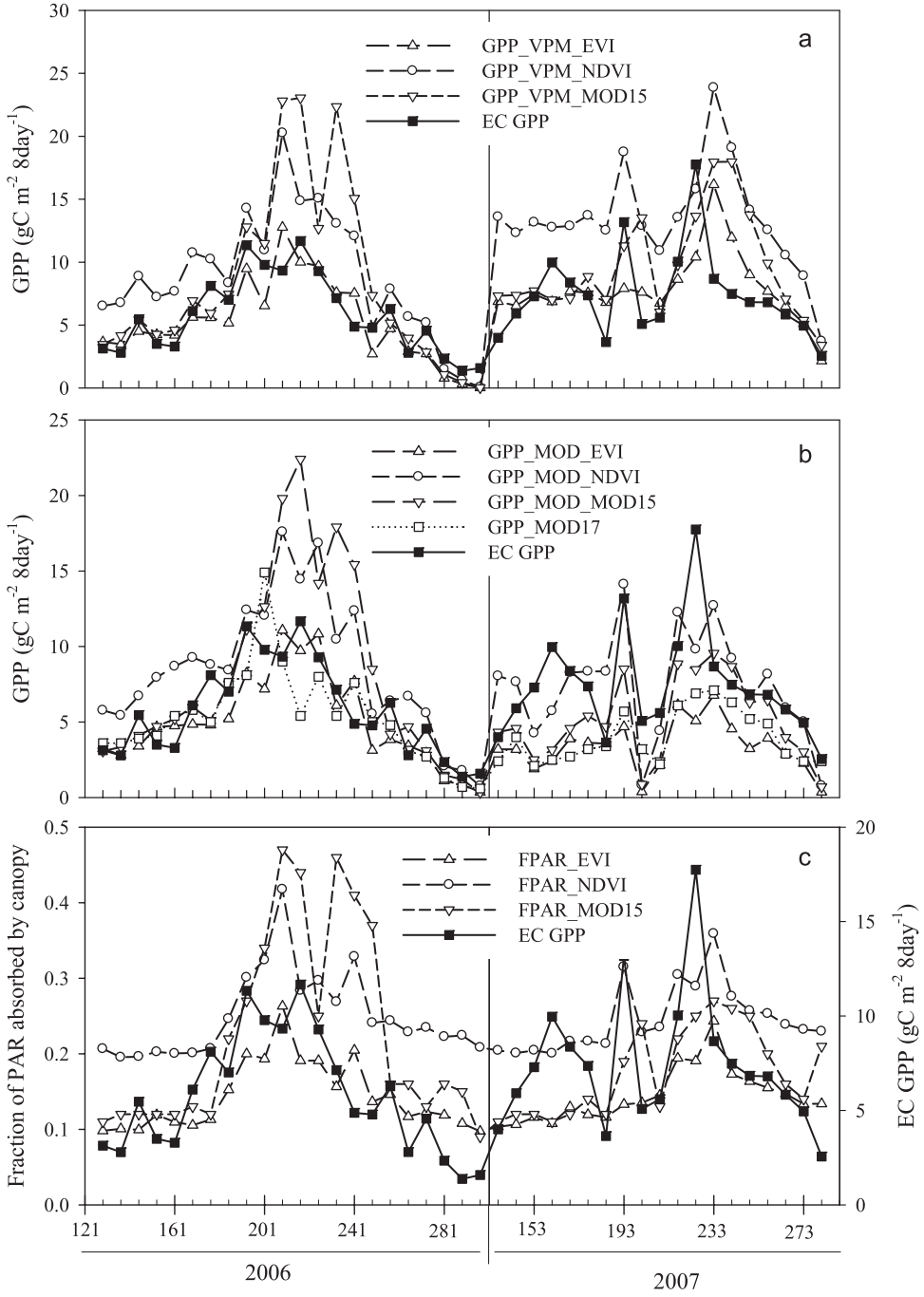

Figure 3: comparison of 8-day EC-measured GPP (EC GPP) with (**a**) the VPM predictions of GPP using various FPAR source, (**b**) the MODIS predictions of GPP using various FPAR source and (**c**) various FPAR estimates.

(C5) according to geographical location of the study site were also underestimated against the EC GPP. Two key sets of variables have significant effects on the prediction of GPP in this study: the environmental multipliers and FPAR estimates. The two remote sensing GPP algorithms differed significantly in the moisture multipliers. The MODIS GPP algorithm utilizes the VPD attenuation function to represent water constraint (Heinsch *et al.* 2006; Zhao *et al.* 2005, 2006), while the VPM applies derivations of the LSWI to reflect land surface moisture. At our study site, GPP was found to strongly depend on soil water content, thus using VPD to reduce radiation efficiency might be inappropriate. VPD and soil moisture have very different characteristics in terms of spatial and temporal dynamics (Hwang *et al.* 2008). Soil moisture has higher spatial variability than VPD due to its strong dependence on topographic gradient, but lower temporal variability than VPD due to its

Table 2: mean 8-day and standard deviation of *GPP* (gC m^{-2} 8-day^{-1}) estimated by the MODIS *GPP* and VPM algorithms with various FPAR estimates and site-specific inputs

GPP methods	Mean (gC m^{-2} 8-day^{-1})	S.D. (gC m^{-2} 8-day^{-1})	R^2	S.E. (gC m^{-2} 8-day^{-1})	Slope (Intercept = 0)
EC *GPP*	6.531	3.386			
VPM_*FPAR_EVI*	6.327	3.472	0.882	2.423	0.959
VPM_*FPAR_NDVI*	10.794	5.444	0.890	2.431	0.575
VPM_*FPAR_MOD15*	8.826	6.068	0.802	3.262	0.618
MODIS_*FPAR_EVI*	4.654	2.569	0.855	2.799	1.282
MODIS_*FPAR_NDVI*	8.843	4.302	0.894	2.386	0.708
MODIS_*FPAR_MOD15*	7.351	5.209	0.786	3.394	0.727
MOD17A2	4.663	2.660	0.806	3.231	1.234

Also shown is the coefficient of determination (adjusted R^2) and standard error of relationships of VPM and MODIS *GPP* with eddy covariance *GPP* (EC GPP).

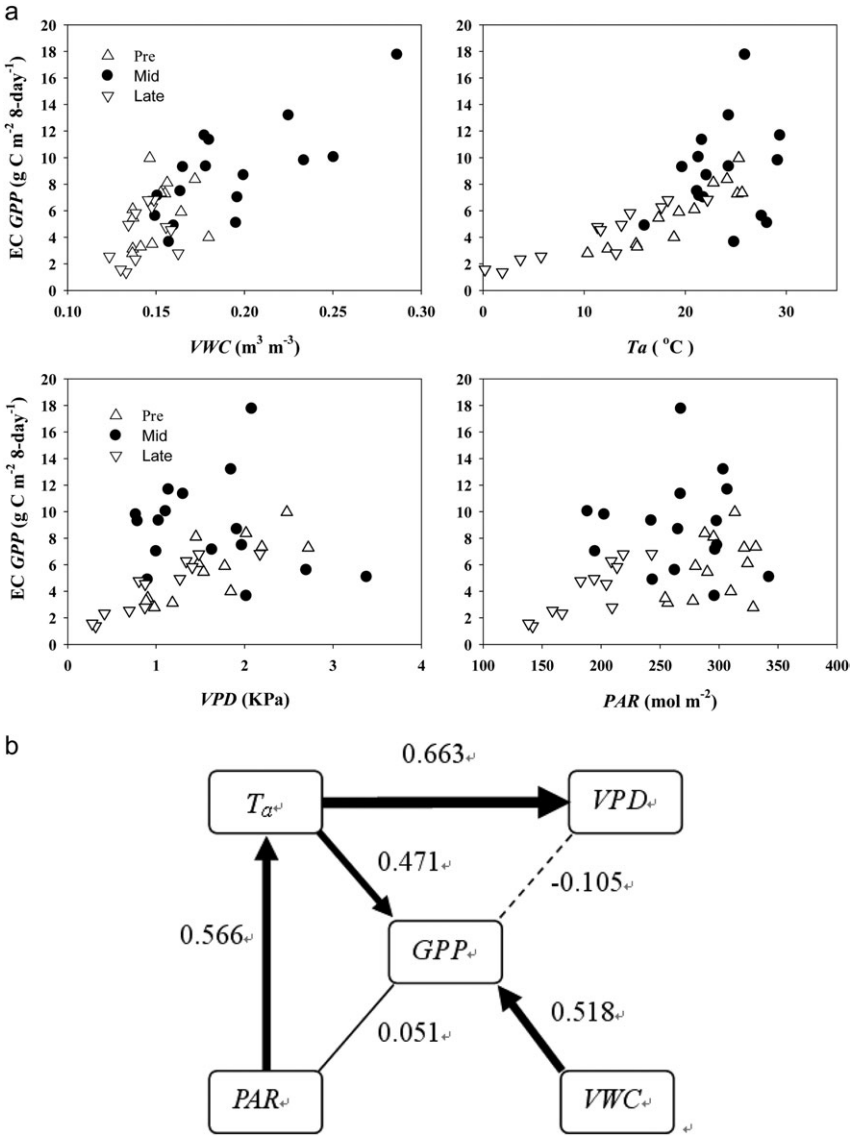

Figure 4: scatter plots (**a**) (△, pre; ●, mid and ▽, late indicate previous, middle and late stage of growing season, respectively) and path diagrams (**b**) illustrating the effects of four major environmental variables, i.e. air temperature at a height of 2 m (T_a), PAR, VWC to a depth of 10 cm and VPD, on ecosystem GPP at a 8 day (**b**) time step at the study site of East Ujimuqin of Inner Mongolia, China. Lines with arrowhead indicate significant effects, and the values are the corresponding path coefficients. Solid lines indicate a positive effect and dashed lines a negative effect.

buffering effect within a soil column. Mu *et al.* (2007) found that atmospheric control cannot capture the seasonality of environmental water stress well in water-limited ecosystems in China. Therefore, a lack of a soil water constraint term in the MODIS GPP algorithm to detect a continuous seasonal drought stress driven by soil water (Turner *et al.* 2005, 2006) may result in significant overestimation of productivity, particularly under extreme drought conditions (Coops *et al.* 2007; Fensholt *et al.* 2006; Leuning *et al.* 2005; Yuan *et al.* 2007). However, the LSWI derived from MODIS has been found useful as an indicator of canopy water stress in the semiarid environment (Fensholt and Sandholt 2003). In this study, the W_{scalar} in VPM derived from the LSWI during the two growing seasons slightly better but not enough to reflect the dynamics of soil water status than the VPD scalar (VPD′) in the MODIS GPP algorithm. Therefore, the use of LSWI as a predictor of water constraint in satellite data-driven primary production modeling appears to be inappropriate in this semi-arid ecosystem, possibly due to that the fraction of vegetation is too low for the index to provide accurate information on canopy water content (Sjöström *et al.* 2009).

FPAR is a key biological property for estimating canopy photosynthesis (Goetz *et al.* 1999; Seaquist *et al.* 2003) because it characterizes vegetation canopy function and energy absorption capacity (Myneni *et al.* 2002, 2003). In this study, we used three types of FPAR estimates, FPAR_EVI, FPAR_NDVI and FPAR_MOD15 and found that the predictions of GPP using either MODIS GPP algorithms or VPM varied with the type of FPAR estimate. FPAR_NDVI and FPAR_MOD15 resulted in GPP overestimation. Through linear regression analysis between EC GPP and three FPAR estimates, we found that FPAR_EVI explained more variations in the EC GPP data than both FPAR_NDVI and FPAR_MOD15. Based on biochemical properties, the FPAR of

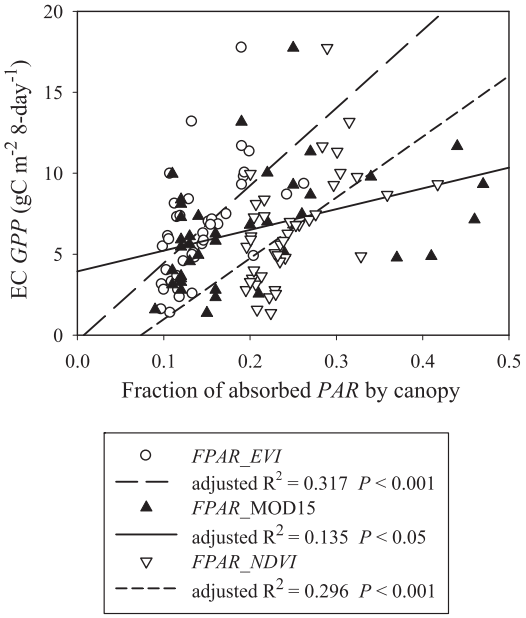

Figure 5: linear relationships of EC GPP with three types of FPAR estimates (i.e. FPAR_EVI, FPAR_MOD15 and FPAR_NDVI) at the study site in East Ujimuqin of Inner Mongolia, China.

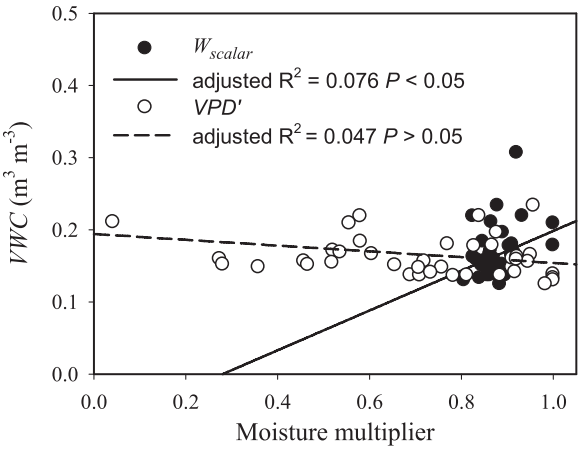

Figure 7: linear relationship between VWC to a depth of 10 cm (m^3 m^{-3}) and the moisture multiplier in the remote sensing algorithms (i.e. T_{scalar} in the VPM and T' in the MODIS GPP algorithm) at the study site in East Ujimuqin of Inner Mongolia, China.

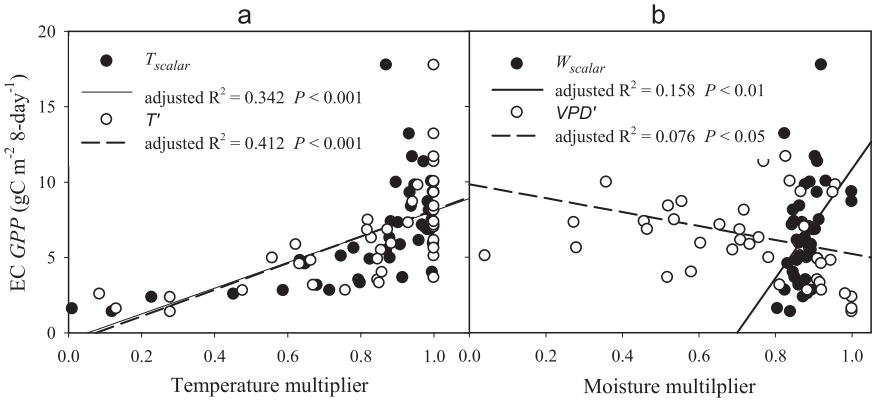

Figure 6: linear relationships of EC GPP with (**a**) the temperature multiplier in the remote sensing GPP algorithms (i.e. T_{scalar} in the VPM and T' in the MODIS GPP algorithm) and (**b**) the moisture multiplier in the remote sensing GPP algorithms (i.e. W_{scalar} in the VPM and VPD′ in the MODIS GPP algorithm) at the study site in East Ujimuqin of Inner Mongolia, China.

vegetation canopy ($FPAR_{canopy}$) can be conceptually partitioned into the fraction of PAR absorbed by chlorophyll ($FPAR_{chl}$) and non-photosynthetic vegetation components ($FPAR_{npv}$) (Xiao *et al.* 2004a; Zhang *et al.* 2005). It has been found that $FPAR_{canopy}$ relates closely to NDVI (Goward and Huemmrich 1992; Zhang *et al.* 2006) and $FPAR_{chl}$ to EVI (Xiao *et al.* 2004a; Zhang *et al.* 2005, 2006). In this study, the FPAR_NDVI or FPAR_MOD15 (MOD15 products) derived from empirical relationships (i.e. the empirical relationship between FPAR and NDVI/LAI) or radiation transfer models (Knyazikhin *et al.* 1999) may lead to GPP overestimation when the same maximum light use efficiency is used over different growing seasons in the two GPP algorithms.

In this study, for the purpose of evaluating the performance of the two remote sensing GPP algorithms, we used the EC GPP measurements of the study site as 'ground truthing'. However, it should be recognized that the EC technique has its limitation and suffers from several technical deficiencies in capturing the real values of ecosystem GPP (Baldocchi 2003; Desai *et al.* 2008; Moffat *et al.* 2007; Stoy *et al.* 2006). Our judgment of the performance of the two GPP algorithms relies on the belief that the EC GPP in this study, after careful quality control/assurance in the data processing, truly reflects the ecosystem GPP while lacking other verifications.

Results in this study indicate that the GPP at the study site of the East Ujimuqin in Inner Mongolia is predominately controlled by soil moisture and temperature. The VPM performs reasonably well in this semiarid grassland ecosystem for integrating the land surface moisture index, whereas a lack of soil moisture modifier in MODIS GPP algorithm may result in GPP overestimation.

FUNDING

National Natural Science Foundation of China (grants 30521002 and 30821062); The 948 program of the State Forestry Administration of China (grant 2006-4-02); NASA-NEWS NN-H-04-Z-YS-005-N program; USCCC program.

ACKNOWLEDGEMENTS

We thank Wenting Xu, Shiping Chen and Jiaqiao Lin for help with maintenance of the flux tower and technical advice on data analysis and the Grassland Work Station of East Ujimuqin Banner of Inner Mongolia for logistic assistance.
Conflict of interest statement. None declared.

APPENDIX: ALGORITHMS FOR GPP

MODIS GPP algorithm

$$GPP_{MOD} = \varepsilon \times FPAR \times PAR, \quad (1)$$

where ϵ is the light use efficiency, FPAR is the fraction of PAR absorbed by the canopy and PAR is the photosynthetic active radiation.

$$\varepsilon = \varepsilon_{max} \times TMIN_{scalar} \times VPD_{scalar}, \quad (2)$$

where ε_{max} is the maximum light use efficiency specific to each biome type, $TMIN_{scalar}$ and VPD_{scalar} are the two simple linear ramp functions calculated as following:

$$TMIN_{scalar} = (TMIN - TMIN_{min})/(TMIN_{max} - TMIN_{min}) \text{ and} \quad (3)$$

$$VPD_{scalar} = (VPD_{max} - VPD)/(VPD_{max} - VPD_{min}), \quad (4)$$

where TMIN is daily minimum temperature, $TMIN_{max}$ and $TMIN_{min}$ are TMIN at $\varepsilon = \varepsilon_{max}$ and $\varepsilon = 0$, VPD is daylight average vapor pressure deficit, VPD_{min} and VPD_{max} are the VPD at $\varepsilon = \varepsilon_{max}$ and $\varepsilon = 0$. When $TMIN_{scalar} > 1$, then $TMIN_{scalar} = 1$; when $TMIN_{scalar} < 0$, then $TMIN_{scalar} = 0$. A similar rule is applicable to VPD_{scalar} for the computation.

For the grass biome in the BPLUT for the MODIS GPP algorithm, the $TMIN_{min}$, $TMIN_{max}$, VPD_{min} and VPD_{max} were defaulted as −8.00°C, 12.02°C, 650 Pa and 3500 Pa, respectively (Heinsch *et al.* 2003).

VPM GPP algorithm

$$GPP_{VPM} = \varepsilon_g \times FPAR_{chl} \times PAR, \quad (5)$$

where ε_g is the light use efficiency and $FPAR_{chl}$ is the fraction of PAR absorbed by leaf chlorophyll in the canopy. In this version of the VPM model, $FPAR_{chl}$ within the photosynthetic active period of vegetation is estimated as a linear function of EVI, and the coefficient a is set at 1.0 (Xiao *et al.* 2004a, 2004b):

$$FPAR_{chl} = a \times EVI. \quad (6)$$

Light use efficiency (ε_g) is affected by temperature, water and leaf phenology:

$$\varepsilon_g = \varepsilon_{max} \times T_{scalar} \times W_{scalar} \times P_{scalar}, \quad (7)$$

where ε_{max} is the apparent quantum yield or maximum light use efficiency, and T_{scalar}, W_{scalar} and P_{scalar} are the scalars for the effects of temperature, water and leaf phenology on light use efficiency of vegetation, respectively (Xiao *et al.* 2004a, 2004b, 2005a, 2005b).

$$T_{scalar} = \frac{(T - T_{min})(T - T_{max})}{[(T - T_{min})(T - T_{max})] - (T - T_{opt})^2}, \quad (8)$$

where T_{min}, T_{max} and T_{opt} are the minimum, maximum and optimal temperature for photosynthetic activities, respectively. If air temperature falls below T_{min}, T_{scalar} is set at zero (Raich *et al.* 1991).

$$W_{scalar} = (1 + LSWI)/(1 + LSWI_{max}), \quad (9)$$

where $LSWI_{max}$ is the maximum LSWI during the growing season for individual pixels. Estimation of site-specific $LSWI_{max}$ is dependent upon the time series of remote sensing data. The

maximum LSWI value for the growing season was selected as an estimate of $LSWI_{max}$ (Xiao *et al.* 2004a, 2004b, 2005a, 2005b). For grassland canopies that have new leaves emerging throughout much of the plant growing season, P_{scalar} is set at 1.0 (Li *et al.* 2007).

REFERENCES

Baldocchi DD (2003) Assessing ecosystem carbon balance: problems and prospects of the eddy covariance technique. *Glob Change Biol* **9**:478–92.

Chapin FS, Matson HPA, Mooney HA. (2002) *Principles of Terrestrial Ecosystem Ecology*. Berlin, Germany: Springer-Verlag, 436.

Coops NC, Jassal RS, Leuning R, *et al.* (2007) Incorporation of a soil water modifier into MODIS predictions of temperate Douglas-fir gross primary productivity: initial model development. *Agric For Meteorol* **147**:99–109.

Desai AR, Richardson AD, Moffat AM, *et al.* (2008) Cross-site evaluation of eddy covariance GPP and RE decomposition techniques. *Agric For Meteorol* **148**:821–38.

Falge E, Baldocchi D, Olson R, *et al.* (2001) Gap filling strategies for defensible annual sums of net ecosystem exchange. *Agric For Meteorol* **107**:43–69.

Fensholt R, Sandholt I. (2003) Derivation of a shortwave infrared water stress index from MODIS near- and shortwave infrared data in a semiarid environment. *Remote Sens Environ* **87**:111–21.

Fensholt R, Sandholt I, Rasmussen MS (2004) Evaluation of MODIS LAI, fAPAR and the relation between fAPAR and NDVI in a semi-arid environment using in situ measurements. *Remote Sens Environ* **91**:490–507.

Fensholt R, Sandholt I, Rasmussen MS, *et al.* (2006) Evaluation of satellite based primary production modeling in the semi-arid Sahel. *Remote Sens Environ* **105**:173–88.

Goetz SJ, Prince SD, Goward SN, *et al.* (1999) Satellite remote sensing of primary production: an improved production efficiency modelling approach. *Ecol Model* **122**:239–55.

Goulden ML, Daube BC, Fan SM, *et al.* (1997) Physiological responses of a black spruce forest to weather. *J Geophys Res Atmos* **102**: 28987–996.

Goward SN, Huemmrich KF (1992) Vegetation canopy PAR absorptance and the normalized difference vegetation index—an assessment using the SAIL model. *Remote Sens Environ* **39**:119–40.

Heinsch FA, Reeves M, Votava P, *et al.* (2003) *User's Guide: GPP and NPP (MOD17A2/A3) Products. NASA MODIS Land Algorithm, version 2.0*. Missoula, MT: School of Forestry, University of Montana, 1–57.

Heinsch FA, Zhao M, Running SW, *et al.* (2006) Evaluation of remote sensing based terrestrial productivity from MODIS using regional tower eddy flux network observations. *IEEE T Geosci Remote* **44**: 1908–25.

Huete A, Didan K, Miura T, *et al.* (2002) Overview of the radiometric and biophysical performance of the MODIS vegetation indices. *Remote Sens Environ* **83**:195–213.

Huete AR, Liu HQ, Batchily K, *et al.* (1997) A comparison of vegetation indices over a global set of TM images for EOS-MODIS. *Remote Sens Environ* **59**:440–51.

Hwang T, Kang S, Kim J, *et al.* (2008) Evaluating drought effect on MODIS gross primary production (GPP) with an eco-hydrological model in the mountainous forest, East Asia. *Glob Change Biol* **14**:1–20.

Huxman TE, Turnipseed AA, Sparks JP, *et al.* (2003) Temperature as a control over ecosystem CO_2 fluxes in a high-elevation, subalpine forest. *Oecologia* **134**:537–46.

Ignace DD, Huxman TE (2009) Limitations to photosynthetic function across season in *Larrea tridentate* (creosotebush) growing on contrasting soil surfaces in the Sonoran Desert. *J Arid Environ* **73**:626–33.

Jin H, Sun OJ, Liu J (2010) Changes in soil microbial biomass and community structure with addition of contrasting types of plant litter in a semiarid grassland ecosystem. *J Plant Ecol* **3**:209–17.

Knyazikhin Y, Glassy J, Privette JL, *et al.* (1999) MODIS leaf area index (LAI) and fraction of photosynthetically active radiation absorbed by vegetation (FPAR) product (MOD15) algorithm theoretical basis document. http://modis.gsfc.nasa.gov/data/atbd/atbd_mod15.pdf (7 July 2011, date last accessed).

Leuning R, Cleugh HA, Zegelin SJ, *et al.* (2005) Carbon and water fluxes over a temperate *Eucalyptus* forest and a tropical wet/dry savanna in Australia: Measurements and comparison with MODIS remote sensing estimates. *Agric For Meteorol* **129**:151–73.

Li CC (1981) *Path Analysis: A Primer*. 3rd edn. Pacific Grove, CA: Boxwood.

Li SG, Eugster W, Asanuma J, *et al.* (2008) Response of gross ecosystem productivity, light use efficiency, and water use efficiency of Mongolian steppe to seasonal variations in soil moisture. *J Geophys Res* **113**:1–13.

Li Z, Yu G, Xiao X, *et al.* (2007) Modeling gross primary production of alpine ecosystems in the Qinghai-Tibet Plateau using MODIS images and climate data. *Remote Sens Environ* **107**:510–19.

Lloyd J, Taylor JA (1994) On the temperature dependence of soil respiration. *Functional Ecology* **8**:315–23.

Moffat AM, Papale D, Reichstein M, *et al.* (2007) Comprehensive comparison of gap filling techniques for eddy covariance net carbon fluxes. *Agric For Meteorol* **147**:209–32.

Monteith JL (1972) Solar radiation and productivity in tropical ecosystems. *J Appl Ecol* **9**:747–66.

Mu Q, Zhao M, Heinsch FA, *et al.* (2007) Evaluating water stress controls on primary production in biogeochemical and remote sensing based models. *J Geophys Res* **112**:G01012.

Myneni R, Knyazikhin Y, Glassy J, *et al.* (2003) *User's Guide fPAR, LAI (ESDT: MOD15A2) 8-day Composite NASA MODIS Land Algorithm, Terra MODIS Land Team*. http://cybele.bu.edu/modismisr/products/modis/userguide.pdf. (28 June 2011, date last accessed).

Myneni RB, Hoffman S, Knyazikhin Y, *et al.* (2002) Global products of vegetation leaf area and fraction absorbed PAR from year one of MODIS data. *Remote Sens Environ* **83**:214–31.

Qin Z, Xu B, Li W, *et al.* (2004) Integration of ground sampling with satellite imaging through GIS database to monitor rangeland productivity for grazing in north China. *Geoinformatics* **2**:715–22.

Raich JW, Rastetter EB, Melillo JM, *et al.* (1991) Potential net primary productivity in South America: application of a global model. *Ecol Appl* **1**:399–429.

Ruimy A, Saugier B, Dedieu G. (1994) Methodology for the estimation of terrestrial net primary production from remotely sensed data. *J Geophys Res Atmos* **99**:5263–83.

Running SW, Nemani RR, Heinsch FA, *et al.* (2004) A continuous satellite-derived measure of global terrestrial 2primary production. *Bioscience* **54**:547–60.

Running SW, Thornton PE, Nemani RR, *et al.* (2000) Global terrestrial gross and net primary productivity from the earth observing system. In: Sala O, Jackson R, Mooney H (eds). *Methods in Ecosystem Science*. New York: Springer, 44–57.

Saito M, Kato T, Tong Y. (2009) Temperature controls ecosystem CO_2 exchange of an alpine meadow on the northeastern Tibetan Plateau. *Glob Change Biol* **15**:221–8.

Sarr DA, Hibbs DE. (2007) Multiscale controls on woody plant diversity in western Oregon riparian forests. *Ecol Monogr* **77**:179–201.

Schlesinger WH, Reynolds JF, Cunningham GI, *et al.* (1990) Biological feedbacks in global desertification. *Science* **247**:1043–8.

Seaquist JW, Olsson L, Ardo J. (2003) A remote sensing-based primary production model for grassland biomes. *Ecol Model* **169**:131–55.

Shao C, Chen J, Li L, *et al.* (2008) Spatial variability in soil heat flux at three Inner Mongolia steppe ecosystems. *Agric For Meteorol* **148**:1433–43.

Sims DA, Rahman AF, Cordova VD, *et al.* (2006) On the use of MODIS EVI to assess gross primary productivity of North American ecosystems. *J Geophys Res* 111: G04015.

Sjöström M, Ardö J, Eklundh L, *et al.* (2009) Evaluation of satellite based indices for gross primary production estimates in a sparse savanna in the Sudan. *Biogeoscience* **6**:129–38.

Stoy PC, Katul GC, Siqueira MBS, *et al.* (2006) An evaluation of models for partitioning eddy covariance-measured net ecosystem exchange into photosynthesis and respiration. *Agric For Meteorol* **141**:2–18.

Tucker CJ (1979) Red and photographic infrared linear combinations for monitoring vegetation. *Remote Sens Environ* **8**:127–50.

Turner DP, Ritts WD, Cohen WB, *et al.* (2005) Site-level evaluation of satellite-based global terrestrial gross primary production and net primary production monitoring. *Glob Change Biol* **11**:666–84.

Turner DP, Ritts WD, Cohen WB, *et al.* (2006) Evaluation of MODIS NPP and GPP products across multiple biomes. *Remote Sens Environ* **102**:282–92.

Wang YL, Zhou GS, Wang YH. (2008) Environmental effects on net ecosystem CO_2 exchange at half-hour and month scales over *Stipa krylovii* steppe in northern China. *Agric For Meteorol* **148**:714–22.

Webb EK, Pearman GI, Leuning R (1980) Correction of flux measurements for density effects due to heat and water vapour transfer. *Q J Roy Meteor Soc.* **106**:85–100.

Whittaker A, Vazzana C, Vecchio V, *et al.* (2009) Evaluation of direct and indirect effects of flavonoids, mineral elements and dry weight on antiradical scavenging activity in leaf material of field-grown *Trifolium pratense* cultivars using Path Analysis. *Field Crop Res* **113**:1–11.

Wilczak JM, Oncley SP, Stage SA. (2001) Sonic anemometer tilt correction algorithms. *Bound Layer Meteorol* **99**:127–50.

Wu JB, Xiao XM, Guan DX, *et al.* (2009) Estimation of the gross primary production of an old-growth temperate mixed forest using eddy covariance and remote sensing. *Int J Remote Sens* **30**:463–79.

Wu WX, Wang SQ, Xiao XM, *et al.* (2008) Modeling gross primary production of a temperate grassland ecosystem in Inner Mongolia, China, using MODIS imagery and climate data. *Sci China Ser D* **51**:1501–12.

Xiao X (2006) Light absorption by leaf chlorophyll and maximum light use efficiency. *IEEE T Geosci Remote* **44**:1933–5.

Xiao X, Boles S, Liu JY, *et al.* (2002) Characterization of forest types in northeastern China, using multi-temporal SPOT-4 VEGETATION sensor data. *Remote Sens Environ* **82**:335–48.

Xiao XM, Hollinger D, Aber J, *et al.* (2004*a*) Satellite-based modeling of gross primary production in an evergreen needle-leaf forest. *Remote Sens Environ* **89**:519–34.

Xiao XM, Zhang QY, Braswell B, *et al.* (2004*b*) Modeling gross primary production of temperate deciduous broadleaf forest using satellite images and climate data. *Remote Sens Environ* **91**:256–70.

Xiao XM, Zhang QY, Hollinger D, *et al.* (2005*a*) Modeling gross primary production of an evergreen needle-leaf forest using MODIS and climate data. *Ecol Appl* **15**:954–69.

Xiao XM, Zhang QY, Saleska S, *et al.* (2005*b*) Satellite-based modeling of gross primary production in a seasonally moist tropical evergreen forest. *Remote Sens Environ* **94**:105–22.

Xie YC, Sha ZY, Yu M. (2008) Remote sensing imagery in vegetation mapping: an overview. *J Plant Ecol* **1**:9–23.

Yan H, Fu Y, Xiao X, *et al.* (2009) Modeling gross primary productivity for winter wheat-maize double cropping system using MODIS time series and CO_2 eddy flux tower data. *Agr Ecosyst Environ* **129**:391–400.

Yan Y, Zhao B, Chen J, *et al.* (2008) Closing the carbon budget of estuarine wetlands with tower-based measurements and MODIS time series. *Glob Change Biol* **14**:1–13.

Yuan W, Liu S, Zhou G, *et al.* (2007) Deriving a light use efficiency model from eddy covariance flux data for predicting daily gross primary production across biomes. *Agric For Meteorol* **143**:189–207.

Zhang F, Zhou GS, Wang YH. (2008) Dynamics simulation of net primary productivity by a satellite data-driven CASA model in Inner Mongolian typical steppe, China. *Chin J Plant Ecol* **32**:786–97.

Zhang QY, Xiao XM, Braswell B, *et al.* (2005) Estimating light absorption by chlorophyll, leaf and canopy in a deciduous broadleaf forest using MODIS data and a radiative transfer model. *Remote Sens Environ* **99**:357–71.

Zhang QY, Xiao XM, Braswell B, *et al.* (2006) Characterization of seasonal variation of forest canopy in a temperate deciduous broadleaf forest, using daily MODIS data. *Remote Sens Environ* **105**:189–203.

Zhao M, Heinsch FA, Nemani RR, *et al.* (2005) Improvements of the MODIS terrestrial gross and net primary production global data set. *Remote Sens Environ* **95**:164–76.

Zhao M, Running SW, Nemani RR. (2006) Sensitivity of moderate resolution imaging spectroradiometer (MODIS) terrestrial primary production to the accuracy of meteorological reanalyses. *J Geophys Res* **111**:G01002.